Molecular circuit involving KLK4 integrates androgen and mTOR signaling in prostate cancer

Yang Jin[a,1], Su Qu[a,1], Martina Tesikova[a], Ling Wang[a], Alexandr Kristian[b], Gunhild M. Mælandsmo[b], Haiying Kong[a], Tianzhou Zhang[a], Carmen Jerónimo[c,d], Manuel R. Teixeira[c,d], Erkan Yuca[e], Ibrahim Tekedereli[e], Kivanc Gorgulu[e], Neslihan Alpay[e], Anil K. Sood[f], Gabriel Lopez-Berestein[e], Håvard E. Danielsen[g,h], Bulent Ozpolat[e], and Fahri Saatcioglu[a,h,2]

[a]Department of Biosciences, University of Oslo, 0316 Oslo, Norway; [b]Department of Tumor Biology, [g]Center for Cancer Biomedicine, and [h]Institute for Medical Informatics, Oslo University Hospital, 0310 Oslo, Norway; [c]Genetics Department and Research Center, Portuguese Oncology Institute, 4200-072 Porto, Portugal; [d]Department of Pathology and Genetics, Biomedical Sciences Institute, University of Porto, 4200-072 Porto, Portugal; and [e]Department of Experimental Therapeutics and [f]Department of Gynecological Oncology, MD Anderson Cancer Center, Houston, TX 77030

Edited* by Michael Karin, University of California, San Diego School of Medicine, La Jolla, CA, and approved May 21, 2013 (received for review March 6, 2013)

The androgen receptor (AR) and the phosphoinositide 3-kinase (PI3K)/protein kinase B/mammalian target of rapamycin (mTOR) signaling are two of the major proliferative pathways in a number of tissues and are the main therapeutic targets in various disorders, including prostate cancer (PCa). Previous work has shown that there is reciprocal feedback regulation of PI3K and AR signaling in PCa, suggesting that cotargeting both pathways may enhance therapeutic efficacy. Here we show that proteins encoded by two androgen-regulated genes, kallikrein related peptidase 4 (KLK4) and promyelocytic leukemia zinc finger (PLZF), integrate optimal functioning of AR and mTOR signaling in PCa cells. KLK4 interacts with PLZF and decreases its stability. PLZF in turn interacts with AR and inhibits its function as a transcription factor. PLZF also activates expression of regulated in development and DNA damage responses 1, an inhibitor of mTORC1. Thus, a unique molecular switch is generated that regulates both AR and PI3K signaling. Consistently, KLK4 knockdown results in a significant decline in PCa cell proliferation in vitro and in vivo, decreases anchorage-independent growth, induces apoptosis, and dramatically sensitizes PCa cells to apoptosis-inducing agents. Furthermore, in vivo nanoliposomal KLK4 siRNA delivery in mice bearing PCa tumors results in profound remission. These results demonstrate that the activities of AR and mTOR pathways are maintained by KLK4, which may thus be a viable target for therapy.

Prostate cancer (PCa) is the most frequently diagnosed cancer in men (1). PCa is initially dependent on androgens for its survival and growth, and thus androgen-deprivation therapy can effectively inhibit tumor growth at this stage. However, most PCa cells eventually progress to a castration resistant stage (CRPC) for which no curative therapy is available. Many factors, such as alterations in androgen receptor (AR) functioning (2–5), loss of tumor-suppressor genes, and oncogenic gene fusions (6) have been implicated in progression to CRPC. Among these factors, AR-mediated androgen signaling pathway has been the most attractive target for therapy against both androgen-dependent and CRPC (7). Both phases of PCa rely on the expression and activity of AR for survival and proliferation, despite significantly lower levels of circulating androgens in the latter (8).

The precise mechanism of CRPC development is not known. However, in addition to AR signaling, the phosphoinositide 3-kinase (PI3K) pathway has strongly been implicated. PI3K signaling plays a critical role in regulating cell growth, differentiation, drug resistance, and survival, and its activation is frequently detected in human cancers (9). Deregulation of this pathway can occur through various processes, such as gain-of-function oncogenic mutations of PIK3CA (PI3K catalytic-α polypeptide) (10) and loss-of-function of the tumor suppressor PTEN (phosphatase and tensin homolog deleted on chromosome 10) (11, 12). PTEN is a negative regulator of the PI3K-protein kinase B (AKT) pathway and it is one of the most highly mutated genes in PCa (13). Loss of one *PTEN* allele is observed in 60–70% of primary tumors, which significantly increases as the disease progresses, and homozygous deletions are associated with advanced disease and metastasis (14, 15). Accordingly, mice with altered dose of *Pten* develop invasive PCa and prostate-specific loss of *Pten* results in invasive and metastatic PCa (13, 15, 16).

A main downstream mediator of the PI3K-AKT pathway is mammalian target of rapamycin (mTOR), which is a serine/threonine kinase that regulates protein synthesis, cell growth, and proliferation through inactivation of eIF4E-binding proteins and activation of ribosomal S6 kinase (S6K) (17–19). Numerous studies suggest that the PI3K/AKT/mTOR pathway is vital to the growth and survival of cancer cells. Consistently, increased AKT activity is associated with higher Gleason grade, advanced disease, and poor prognosis of PCa (20, 21).

mTORC activity is regulated by several molecules, one of which is regulated in development and DNA damage responses 1 (REDD1) (17). It has been suggested that REDD1 inhibits mTORC1 by regulating the release of tuberous sclerosis 2 protein (TSC2) from its association with 14-3-3, which stabilizes TSC1–TSC2 interaction, an inhibitory complex for mTORC1 (22, 23). Many insults from the environment can regulate REDD1 expression, suggesting that it has a broad role in relaying stress signals to mTORC1 (17).

Significance

All cancer lesions sustain alterations in signaling pathways, which are the drivers of disease initiation and progression. Study of altered signaling in cancer is thus important to develop more effective therapeutic regimens as well as better prognostic markers. In this study, we show that two of the most frequently altered signaling pathways in prostate cancer, the androgen receptor and the phosphoinositide 3-kinase/protein kinase B/mammalian target of rapamycin pathways, are dependent on kallikrein related peptidase 4 (KLK4), whose expression is highly prostate enriched. Our results suggest that KLK4 has a central role in prostate cancer survival and that KLK4 silencing may have significant therapeutic efficacy.

Author contributions: Y.J., S.Q., B.O., and F.S. designed research; Y.J., S.Q., M.T., L.W., A.K., T.Z., E.Y., I.T., K.G., and N.A. performed research; C.J., M.R.T., A.K.S., G.L.-B., and H.E.D. contributed new reagents/analytic tools; Y.J., S.Q., G.M.M., H.K., B.O., and F.S. analyzed data; and Y.J., S.Q., B.O., and F.S. wrote the paper.

The authors declare no conflict of interest.

*This Direct Submission article had a prearranged editor.

[1]Y.J. and S.Q. contributed equally to this work.

[2]To whom correspondence should be addressed. E-mail: fahris@ibv.uio.no.

This article contains supporting information online at www.pnas.org/lookup/suppl/doi:10.1073/pnas.1304318110/-/DCSupplemental.

AR activation regulates a large cluster of genes involved in multiple aspects of cellular function. Genome-wide explorations have revealed that several hundred genes are primary targets of AR in lymph node carcinoma of the prostate (LNCaP) PCa cells (24, 25). Kallikrein-related peptidase 4 (KLK4) was previously identified as an androgen-regulated gene (25–27). Previous studies have shown that KLK4 is expressed in the prostate epithelium and is significantly overexpressed in PCa compared with benign prostate (26, 28–30). Ectopic expression of KLK4 in PCa cells resulted in increased cell mobility (29, 31) and increased cell proliferation (29). We have previously shown that ectopic expression of KLK4 promotes PCa cell proliferation, at least in part, by regulating cell-cycle gene expression (29). Although these observations have shown that overexpression of KLK4 has an important role in PCa progression, it is not clear as to how KLK4 modulates cell growth in PCa cells and whether it can serve as a therapeutic target.

Another androgen-regulated gene that has been implicated in development and cancer is promyelocytic leukemia zinc finger protein (PLZF; also known as Zbtb16 or Zfp145) (32). Originally identified in acute promyelocytic leukemia, this gene belongs to a family of transcriptional repressors and has been implicated in a variety of developmental and biological processes, including serving as a tumor-suppressor gene (32). Despite its androgen regulation, the role of PLZF in PCa, if any, is not known.

Here we provide evidence for a molecular switch involving direct interactions between KLK4 and PLZF in PCa cells. We find that PLZF binds to and inhibits AR. In addition, PLZF inhibits mTORC1 signaling through activation of REDD1 expression. Through direct interactions, KLK4 inhibits PLZF action and thereby keeps the AR and mTORC1 signaling active. Consistently, KLK4 knockdown greatly decreases PCa growth in vitro and in vivo, suggesting that it could be a bona fide therapeutic target for PCa.

Results

KLK4 Knockdown Inhibits Cell Growth. To explore the possible mechanisms of KLK4-induced cell growth, we established LNCaP cell lines stably expressing three independent short hairpin RNAs (shRNAs) directed against KLK4 using lentiviral gene delivery. All KLK4 shRNAs efficiently decreased R1881-induced KLK4 expression at both the mRNA and protein levels (Fig. S1 *A* and *B*). shKLK4#1, which was most effective for KLK4 knockdown, had similar activity in Los Angeles prostate cancer 4 (LAPC4) and vertebral carcinoma of the prostate (VCaP) cells, two independent androgen-responsive PCa cell lines (Fig. S1 *C* and *D*).

We then determined the possible effect of sustained KLK4 knockdown on PCa cell growth in vitro. As shown in Fig. 1*A*, the KLK4-depleted cells (LN-shKLK4, expressing shKLK4#1) had significantly reduced growth rates compared with control cells (LN-Scr) that stably express a shRNA with a scrambled (Scr) sequence. Similar results were obtained in LAPC4 cells (Fig. 1*B*). Furthermore, KLK4-depleted LNCaP and LAPC4 cells formed ~80–90% fewer colonies compared with control cells in a soft-agar assay, indicating a decrease in anchorage-independent growth (Fig. 1 *C* and *D*). Qualitatively similar results were obtained using two independent shRNAs (Fig. S1*E*). Expression of shKLK4#1, which most efficiently knocks down KLK4 expression (Fig. S1 *A* and *B*), was also the most effective in suppressing cell growth (Fig. S1*E*). Consistently, KLK4 knockdown significantly reduced the colonigenic potential of VCaP cells by 60% (Fig. 1*E*). These data, obtained in three independent PCa cell lines, indicate that KLK4 makes a significant contribution to PCa cell growth in vitro.

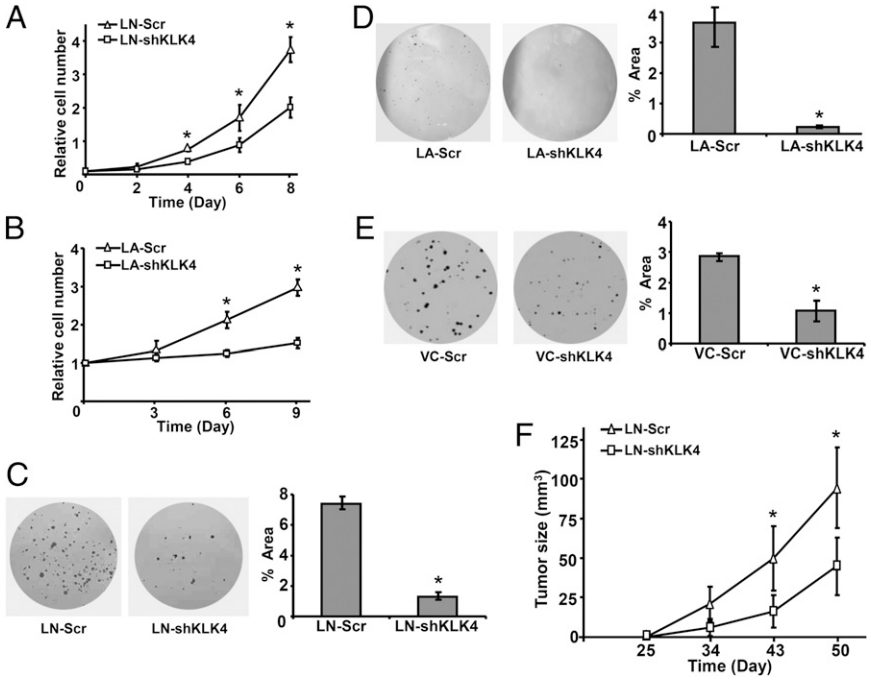

Fig. 1. Knockdown of KLK4 inhibits PCa cell growth in vitro and in vivo. (*A*) Growth analysis of KLK4 knockdown in LNCaP cells. LN-Scr and LN-shKLK4 cells were seeded in six-well plates in regular growth medium and cell growth was determined by direct cell counting in a hemocytometer at 2-d intervals. (*B*) KLK4 knockdown effects on LAPC4 cell growth. LA-Scr (control) and LA-shKLK4 (knockdown) cells were seeded in six-well plates in regular growth medium and the growth of each line was determined by direct cell counting every 3 d. (*C* and *D*) KLK4 knockdown inhibits anchorage-independent growth of LNCaP and LAPC4 cells. The soft-agar colony formation of LNCaP (*C*) and LAPC4 cells (*D*) was assessed with or without KLK4 knockdown as described in *Materials and Methods*. The area covered by colonies was quantified. (*E*) KLK4 knockdown inhibits clonogenic capacity of VCaP cells. VC-Scr (control) or VC-shKLK4 (knockdown) cells were cultured for 3 wk. The colonies formed were stained with Crystal violet and photographed. The area covered by colonies was quantified. (*F*) Growth analysis of xenografted LNCaP tumors in NOD/SCID mice. LNCaP cells expressing shRNA against KLK4 or control shRNA were subcutaneously implanted into both flanks of five male NOD/SCID mice. Tumor size was measured at the indicated time points. Error bars for cell number and clonogenic assay indicate SD ($n = 3$), and for tumor size indicate SEM. *$P < 0.05$. Data shown in *A–E* are from a representative experiment repeated three times with similar results.

To check the validity of these findings in vivo, we performed xenograft experiments. Equal numbers of LN-shKLK4 and LN-Scr cells were subcutaneously injected into nonobese diabetic (NOD)/SCID mice, allowed to grow, and tumor sizes were monitored over time. Both cell lines formed tumors, but LN-shKLK4 xenografts grew significantly slower compared with LN-Scr xenografts (Fig. 1*F*). We have confirmed that in the emergent tumors from LN-shKLK4 cells knockdown levels of KLK4 expression persisted during tumor growth (Fig. S1*F*), indicating that in these stably transduced cells KLK4 knockdown alone is not sufficient to halt tumor growth completely, perhaps because of some compensatory mechanisms. These data show that KLK4 knockdown inhibits PCa tumor growth in vivo.

KLK4 Knockdown Induces G1 Arrest and Increases Cell Death. Our previous work has shown that ectopic expression of KLK4 affected cell-cycle regulator gene expression in the PCa cell line PC3 (29). Because the above data clearly implicated KLK4 in cell growth, we examined possible alterations in cell-cycle progression upon KLK4 depletion using flow cytometry. LN-shKLK4 cells had a significant increase in G1 and subG1, as well as a decrease in both S and G2-M phases, compared with LN-Scr cells (Fig. S2*A*). These data indicated that KLK4 knockdown significantly delayed cell-cycle progression as well as increasing cell death.

To assess whether KLK4 knockdown-induced cell death involved apoptosis, we used the TUNEL assay. Significantly higher apoptosis was detected in LN-shKLK4 cells compared with control cells (Fig. S2 *B* and *C*). We then examined the susceptibility of LN-shKLK4 cells to apoptosis inducers compared with LN-Scr cells. To that end, we used TNF-related apoptosis-inducing ligand (TRAIL), which induces apoptosis in PCa cells (33). However, LNCaP cells are resistant to TRAIL-induced apoptosis because of constitutively active AKT, similar to that frequently seen in PCa in situ, and TRAIL+PI3K inhibitors can be used to overcome this resistance (34). We thus treated the cells with either TRAIL or a PI3K inhibitor (LY294002) either alone or in combination, and determined the extent of apoptosis. As shown in Fig. S2*B*, similar to untreated cells, KLK4 knockdown significantly increased cell death in response to TRAIL or LY294002, reaching ∼8% cell death. When the two agents were used together, there was a dramatic increase in LN-shKLK4 cell sensitivity to apoptosis, which was approximately sixfold higher than that observed in control cells where the extent of cell death reached >60% (Fig. S2 *B* and *C*). Consistent with this picture, there was a significant increase in caspase 3 and poly(ADP-ribose) polymerase (PARP) cleavage upon KLK4 knockdown under all conditions tested (Fig. S2*D*). Sensitization to TRAIL+LY294002-mediated apoptosis upon KLK4 depletion was also observed in LAPC4 cells, indicated by the cleavage of caspase-3 and PARP (Fig. S2*E*). These results show that KLK4 is a potent antiapoptotic factor in PCa cells and its knockdown dramatically increases sensitivity to apoptosis.

KLK4 Knockdown Suppresses AR Signaling. AR plays an important role in PCa development by increasing proliferation and inhibiting apoptosis and is critical in CRPC (7, 35). To test whether KLK4 may modulate AR activity, we cultured LN-shKLK4 or LN-Scr cells in the presence or absence of R1881 and examined the expression of well-established AR-regulated genes. In LN-shKLK4 cells, in addition to KLK4, there was a significant reduction of androgen-induced prostate-specific antigen (PSA) and transmembrane protease serine 2 (TMPRSS2) expression compared with LN-Scr cells (Fig. 2*A*), and even a greater reduction at the protein level (Fig. 2*B*). Similar effects were observed in LNCaP cells expressing independent KLK4 shRNAs (Fig. S3 *A* and *B*). Consistently, experiments in LAPC4 and VCaP cells stably expressing KLK4 shRNA showed that KLK4 has similar effects on AR target gene expression in these cells (Fig. S3 *C* and *D*). In contrast, KLK4 knockdown did not have any effect on growth characteristics of an androgen-independent PCa cell line (DU145), in which neither AR nor KLK4 is expressed, indicating that KLK4 effects in PCa cells are mediated, at least in part, by its effects on AR signaling (Fig. S3*E*). To determine if KLK4 affects AR transcriptional activity, we transiently introduced an AR dependent reporter, -285-PB-LUC, into the LN-shKLK4 and LN-Scr cells and determined its response to R1881. As shown in Fig. 2*C*, there was a >80% reduction in AR transcriptional activity in LN-shKLK4 cells compared with LN-Scr cells. These data suggest that KLK4 is required for AR activity and/or its production or stability.

Immunofluorescence microscopy showed that AR accumulated in the nucleus of both LN-shKLK4 and LN-Scr cells, but AR levels were significantly decreased in LN-shKLK4 cells (Fig. S4*A*). This finding indicated that KLK4 knockdown resulted in reduced AR protein expression, which was verified by Western analysis (Fig. 2*D*) and was confirmed with independent shRNAs (Fig. S4*B*). A time-course experiment in the presence of protein synthesis inhibitor cycloheximide showed that AR protein stability was not significantly affected upon KLK4 knockdown (Fig. S4*C*). We thus assessed steady-state *AR* mRNA levels by quantitative PCR (qPCR) and observed a significant decline in LN-shKLK4 cells compared with LN-Scr cells at all time points of R1881 treatment (Fig. S4*D*). There were similar effects on AR expression upon KLK4 knockdown in LAPC4 cells at both mRNA and protein levels (Fig. S4 *E* and *F*). These data show that KLK4 is required for steady-state AR levels in PCa cells.

To determine if the effect of KLK4 on AR signaling extends to human PCa samples, we evaluated possible correlation between *KLK4* expression and global AR target-gene expression that was recently identified by ChIP-Seq experiments in LNCaP cells (36). We first classified *KLK4* status as high and low in a cohort of 281 PCa patient samples for which global mRNA expression data are available (37). We then investigated possible correlations between *KLK4* expression and AR target gene expression in these samples and found that they were highly correlated (Table S1). These data support the findings from above and show that KLK4 is linked to androgen signaling in vivo.

KLK4 Knockdown Inhibits p70S6K Activation. In addition to AR signaling, dysregulation of multiple mitogenic signaling pathways are implicated in PCa development (38, 39). To determine whether the effects of KLK4 knockdown on PCa cells are exclusively dependent on AR signaling, we measured LN-shKLK4 cell growth in the presence or absence of androgens. LN-shKLK4 cells had significantly diminished survival potential compared with LN-Scr cells even in the absence of androgen (Fig. S5*A*). This finding indicated that inhibition of cell proliferation and increase in apoptosis observed upon KLK4 knockdown may involve other pathways in addition to androgen signaling. Three of the most central signaling pathways relevant for PCa are the EGF, PI3K/AKT/mTORC, and NF-κB pathways (38, 39). We thus determined if KLK4-mediated effects on PCa cells involve any changes in the activity of these pathways (Fig. 2*E* and Fig. S5*B*). The basal levels of ERK1/2, a downstream readout for the EGF pathway, were weak and its activation by serum stimulation was not significantly altered by KLK4 knockdown. p65 was not activated by serum and the basal levels did not change upon KLK4 knockdown (Fig. S5*B*). In contrast, serum stimulation of p70S6K phosphorylation, a target of mTORC1, was dramatically decreased in LN-shKLK4 cells (Fig. 2*E*), as well as mTORC1 activation (Fig. S5*C*). Interestingly, Akt activation, which is upstream of mTORC1, was not affected (Fig. S5*D*). The significant decrease in p70S6K activation in KLK4-knockdown cells was also observed in growth medium supplemented with charcoal-stripped serum (Fig. S5*E*), indicating that this effect is not significantly affected by androgen signaling. KLK4-depletion similarly affected p70S6K activation in LNCaP cells expressing independent KLK4 shRNAs (Fig. S5*F*), as well as in LAPC4 cells (Fig. S5*G*). In addition, ectopic

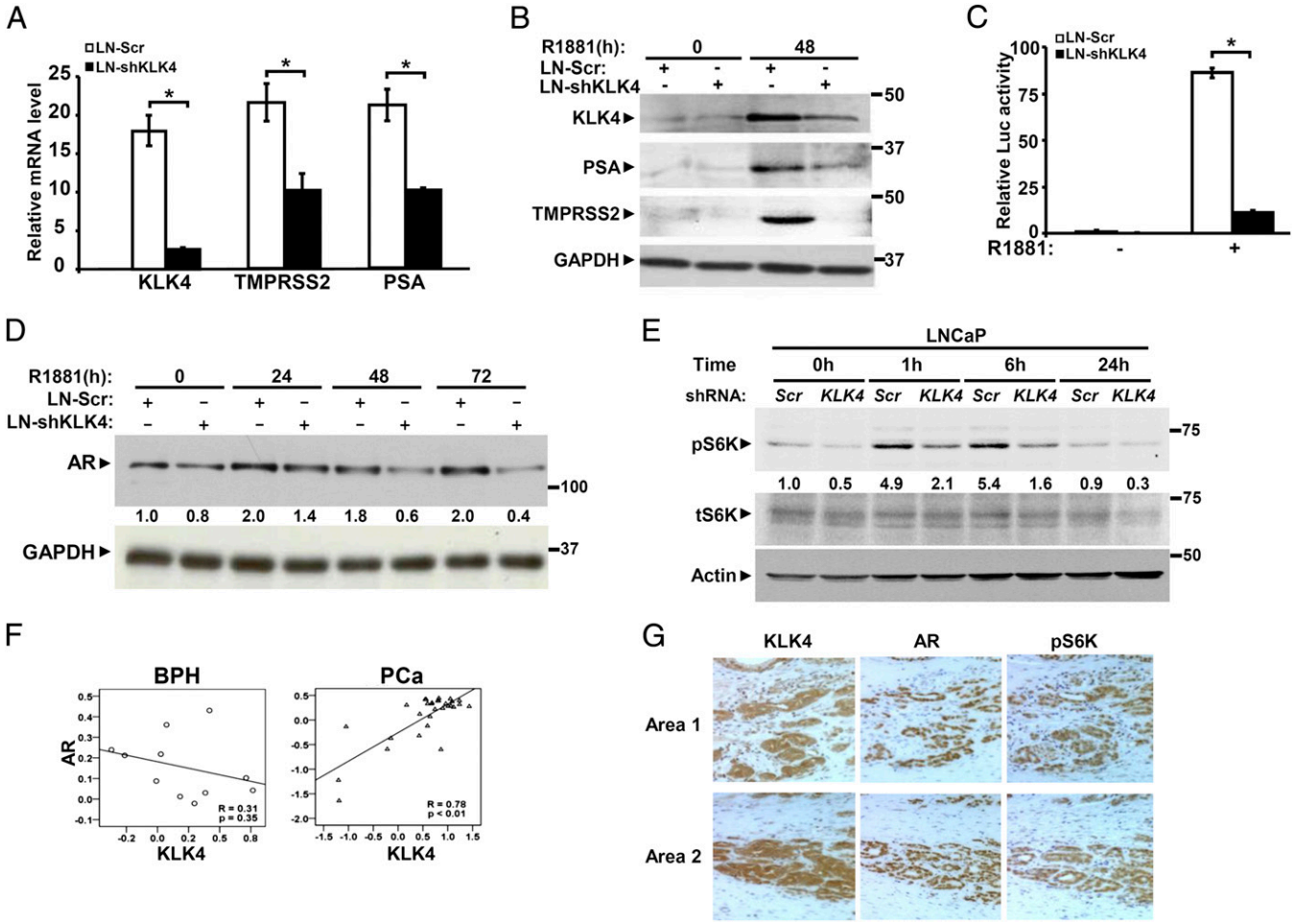

Fig. 2. KLK4 knockdown suppresses AR signaling. (*A*) qPCR analysis of *KLK4, PSA,* and *TMPRSS2* mRNA expression in LN-Scr and LN-shKLK4 (LN-shKLK4, expressing shKLK4#1) cells in the presence of R1881. Error bars indicate SD ($n = 3$); $^*P < 0.05$. (*B*) LN-Scr and LN-shKLK4 cells were left untreated or treated with R1881 for 48 h followed by Western analysis using the indicated antisera. (*C*) AR-dependent reporter gene activity upon KLK4 knockdown in LNCaP cells. AR-dependent reporter -285-PB-LUC was introduced into the LN-Scr and LN-shKLK4 cells by transient transfection. Cells were then either left untreated or treated with R1881 and LUC expression was determined. Error bars indicate SD ($n = 3$); $^*P < 0.05$. (*D*) AR expression in LN-Scr and LN-shKLK4 cells was determined by Western analysis. LN-Scr and LN-shKLK4 cells were either left untreated or treated with R1881 for the indicated time points. Relative quantification of band intensities are indicated below the lanes; Scr at $t = 0$ was set to 1.0. (*E*) LN-Scr and LN-shKLK4 cells were maintained in normal growth medium. After addition of new medium (RPMI with 10% FBS) for the indicated time points, cells were harvested and used in Western analysis with phospho-p70S6K (pS6K) and total-p70S6K (tS6K) antibodies. Anti-actin antiserum was used to evaluate loading. Relative quantification of band intensities are indicated below the lanes; Scr at $t = 0$ was set to 1.0. (*F*) Regression analysis of KLK4 and AR expression in BPH and PCa lesions. 11 BPH and 34 PCa specimens that were snap frozen upon resection were used to analyze *AR* and *KLK4* expression by qPCR. The correlation in expression (Log_2 values) was plotted. The regression line between two genes is drawn as a solid line. The *R* and *P* values are listed in each panel. (*G*) Representative immunostaining of human PCa specimens showing coexpression of AR, KLK4, and pS6K. Consecutive sections of formalin fixed and paraffin embedded human PCa prostatectomy samples were immunostained with antisera against AR, KLK4 or pS6K as indicated. (Magnification: 200×.) Two representative areas are shown. All experiments were repeated at least three times with similar results.

expression of both wild-type KLK4, and a KLK4 mutant (S195A), in which the catalytic triad is inactivated, resulted in activation of S6K phosphorylation (Fig. S6*A*), indicating that observed effects are independent of KLK4 protease activity. These data show that androgen deprivation phenocopies KLK4 knockdown and ectopic KLK4 expression rescues effects on S6K activation.

We used the same approach to determine the consequences of ectopic KLK4 expression on AR signaling. As shown in Fig. S6 *B–D*, expression of either the wild-type KLK4 or the S195A mutant significantly increased expression of AR target genes PSA, TMPRSS2, and six transmembrane prostate protein 2 (STAMP2). These data are consistent with those from above and further show that KLK4 protease activity is not required for its effects on androgen signaling.

The data presented above demonstrated that loss of KLK4 significantly attenuated AR expression in PCa cells, indicating that KLK4 provides a positive feedback loop on AR signaling, which may be relevant for in situ disease. To investigate if the positive correlation between KLK4 and AR expression observed in PCa cell lines exists in patient samples, we compared *AR* and *KLK4* mRNA levels in benign prostate hyperplasia (BPH) and PCa samples that were quickly frozen and preserved upon resection. As shown in Fig. 2*F*, there was a significant positive correlation of *AR* and *KLK4* mRNA expression in PCa, but not in BPH samples, consistent with the increased levels of AR and KLK4 in PCa compared with normal prostate (4, 26, 29, 40). The fact that the correlation is not present in BPH samples suggests that there may be a threshold for AR and KLK4 levels before such interactions would take place, or that there are differences in the way AR and KLK4 expression may be impacted in these tissues. These data, together with those provided above, suggest that there is a positive feedback loop between AR and KLK4.

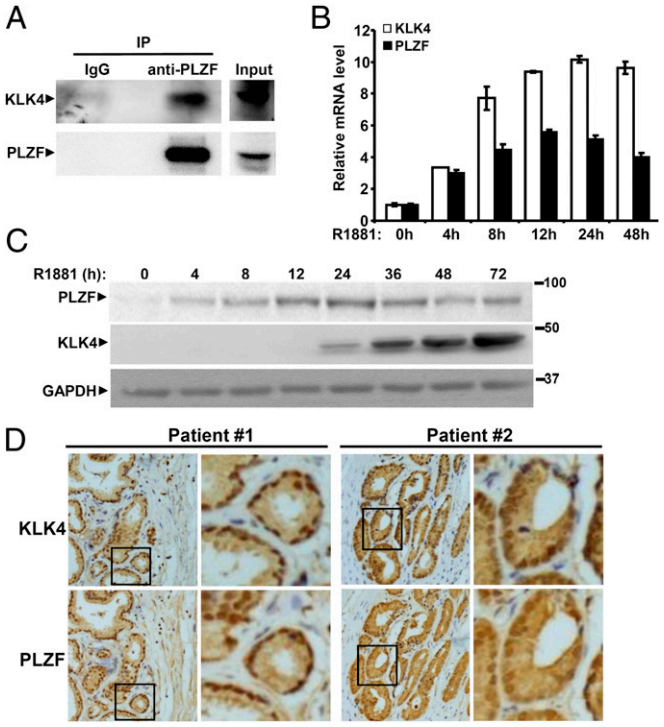

Fig. 3. KLK4 interacts and is coexpressed with PLZF. (*A*) KLK4 interacts with PLZF in vivo. Immunoprecipitation was conducted in LNCaP cells using PLZF antiserum or rabbit IgG. Precipitated fractions were subjected to Western analysis using a KLK4 antiserum. The experiment was repeated two times with similar results. (*B* and *C*) KLK4 and PLZF expression in response to androgen stimulation in LNCaP cells were determined by qPCR (*B*) or Western (C) analysis. Error bars indicate SD (n = 3); *P < 0.05. (*D*) Representative immunostaining showing coexpression of KLK4 and PLZF in consecutive sections of human PCa tumor specimens. (Magnification: 200×.) Boxed areas are enlarged approximately 3× and presented to the right of each image.

To assess whether this correlation extends to the protein level, serial sections of human prostatectomy samples were examined by immunohistochemistry for KLK4, AR, and pS6K. As shown in Fig. 2*G* and Fig. S7, there was clear colocalization of AR, KLK4, and pS6K expression in human PCa specimens. These results are consistent with the data provided above and suggest the presence of a network of interactions between KLK4, AR, and mTOR signaling in PCa.

KLK4 Interacts and Coexpresses with PLZF in PCa Cells. To identify proteins that may mediate the KLK4 effects documented above, we used the yeast two-hybrid system, which identified PLZF as a putative interacting partner of KLK4. This interaction was confirmed by coimmunoprecipitation (co-IP) analysis of COS-7 cells transfected with HA-tagged KLK4 and His-tagged PLZF (Fig. S8*A*), as well as in LNCaP cells with the endogenous proteins (Fig. 3*A*).

PLZF is a 673-amino acid transcriptional regulator that belongs to a large protein family characterized by an N-terminal broad-complex, tramtrack, and bric à brac domain (BTB), a repression domain 2 (RD2), and a C-terminal zinc finger domain (41). To determine which domain of PLZF is involved in interaction with KLK4, two truncated forms of PLZF were made and examined in a co-IP experiment. As shown in Fig. S8*B*, in addition to full-length PLZF, interaction with KLK4 was observed for the deletion mutant amino acids 197–673, but not amino acids 1–313, indicating that the BTB/POZ domain of PLZF is not required for interaction with KLK4. Conversely, we found that two KLK4 isoforms which differ from the wild-type KLK4 in the C-terminal half (27) could interact with PLZF (Fig. S8*C*), indicating that the main PLZF interaction domain of KLK4 resides in its N-terminal half.

qPCR and Western analysis showed that both KLK4 and PLZF are regulated by androgens in LNCaP cells at the mRNA and protein levels (Fig. 3 *B* and *C*), consistent with previous findings (26, 42). Interestingly, the *PLZF* mRNA levels increased until 12 h and thereafter declined as KLK4 mRNA levels continued to increase (Fig. 3*B*). This negative correlation between PLZF and KLK4 at later time points was even more significant at the protein level (Fig. 3*C*). Furthermore, immunohistochemical staining of consecutive sections from human PCa specimens showed that KLK4 and PLZF are colocalized (Fig. 3*D* and Fig. S9). These data suggest that there may be functional interactions between KLK4 and PLZF in PCa.

KLK4 Regulates PLZF Stability. As shown above (Fig. 3 *B* and *C*), and consistent with previous reports (26, 42), both KLK4 and PLZF expression are regulated by androgens in LNCaP cells. Furthermore, PLZF and KLK4 protein levels were negatively correlated (Fig. 3*C*). We therefore asked whether KLK4 regulates PLZF protein stability. To this end, we evaluated the possible effect of KLK4 knockdown on PLZF that is ectopically expressed in LNCaP cells. As shown in Fig. 4*A*, upon KLK4 knockdown PLZF levels significantly increased compared with control siRNA treated cells. Similarly, there was a significant increase in the level of ectopically expressed PLZF upon KLK4 knockdown (Fig. 4*B*). Examination of PLZF levels in the presence of protein synthesis

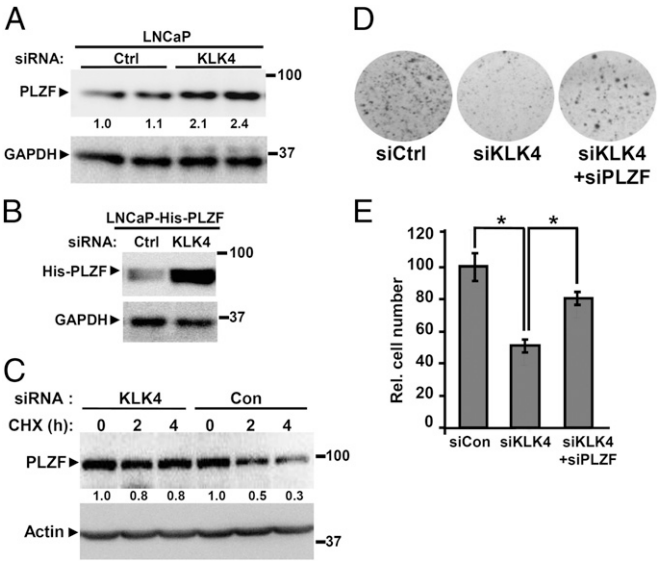

Fig. 4. KLK4 knockdown stabilizes PLZF levels. (*A* and *B*) Either parental LNCaP cells (*A*) or LNCaP cells expressing His tagged PLZF (*B*) were transfected with control (Ctrl) siRNA or siRNA targeting KLK4 and treated with R1881 for 24 h. The cells were then harvested and PLZF expression was examined by Western analysis. Relative quantification of band intensities are indicated below the lanes; the sample in the first lane of Ctrl siRNA was set to 1.0. (*C*) LNCaP cells were transfected with control siRNA or KLK4 siRNA. One day after transfection, cells were stimulated with 10 nM R1881 for 24 h. The cells were then treated with 50 μg/mL cycloheximide (CHX) for the indicated times. The PLZF protein level was determined by Western analysis. Relative quantification of band intensities are indicated below the lanes; CHX at t = 0 was set to 1.0. (*D*) Knockdown of PLZF rescues KLK4-depletion induced cell growth inhibition. LNCaP cells were transfected with, scrambled siRNA (siCtrl), siRNA against KLK4 (siKLK4), or siRNAs against KLK4 and PLZF (siKLK4+siPLZF). Cell growth was assessed by colony-forming assay. (*E*) Quantification of data presented in *D*. Error bars indicate SD (n = 3); *P < 0.05. Data shown in *A*–*E* are from a representative experiment repeated three times with similar results.

inhibitor cycloheximide showed that KLK4 inhibits PLZF protein stability (Fig. 4*C*). These results show that androgen-induced PLZF expression is negatively regulated by KLK4.

PLZF was previously associated with inhibition of cancer cell growth (43). Therefore, we assessed the possible effect of PLZF on growth inhibition of PCa cells induced by KLK4 knockdown. Depletion of PLZF in LNCaP cells significantly rescued KLK4 knockdown-induced growth inhibition (Fig. 4 *D* and *E*), indicating that PLZF is involved in KLK4 regulation of cell growth.

PLZF Is Required for KLK4 Effects on AR Signaling. PLZF was previously associated with inhibition of cancer cell growth (43). We therefore considered the possibility that through direct interactions, KLK4 inhibits PLZF tumor-suppressor activity. To assess this possibility, we used siRNA to knock down PLZF in LN-shKLK4 cells and thereafter assessed any changes in AR signaling. As shown in Fig. 5 *A* and *B*, PLZF siRNA treatment decreased PLZF levels >80% in the presence or absence of R1881. Upon PLZF knockdown, the expression of the AR target gene TMPRSS2 was significantly increased. Similar observations were made when PLZF expression was knocked down in parental LNCaP cells (Fig. 5*C*). Taken together, these data showed that KLK4 effects on AR signaling are mediated, at least in part, by PLZF.

To further address the mechanisms by which PLZF suppresses androgen-regulated gene expression, we generated LNCaP cell lines that stably express His-PLZF or GFP as a control (Fig. S10*A*). Ectopic expression of His-PLZF significantly suppressed the expression of AR target genes *PSA* and *TMPRSS2*, as well as *KLK4* (Fig. S10*B*). Ectopic expression of PLZF did not significantly affect AR mRNA (Fig. S10*B*) or protein levels (Fig. S10*C*), indicating that AR suppression by PLZF is predominantly on its transcriptional activity. Consistently, PLZF inhibited AR transactivation of the 285-PB-LUC reporter (Fig. S10*D*). To determine whether this effect could be because of changes in AR association with its targets in chromatin, we performed ChIP assays. Ectopic expression of PLZF significantly decreased AR binding to the androgen-responsive elements associated with the *PSA* and *TMPRSS2* genes (Fig. 5*D*). These data indicate that PLZF inhibits AR transcriptional activity, at least in part, by inhibiting AR binding to its response elements in vivo.

We then considered the possibility that the inhibitory effects of PLZF on AR could be caused by direct protein–protein interactions. To assess this hypothesis, we used co-IP experiments in LNCaP cells. As shown in Fig. 5*E*, AR readily interacted with the endogenous PLZF in LNCaP cells in an androgen dependent manner. Similar results were obtained with ectopically expressed His-PLZF and endogenous AR in LNCaP cells (Fig. S10*E*). These data suggest that the effects of PLZF on AR are mediated by direct AR–PLZF interactions.

PLZF Is Required for REDD1 Expression in PCa Cells. As shown above (Fig. 2*E*), KLK4 knockdown significantly reduced mTORC1 activity. However, there was no significant change in pAKT levels, an upstream effector of mTORC1, suggesting that the alteration in mTORC1 activity by KLK4 knockdown is independent of the PI3K-AKT pathway. Recent results suggested that PLZF opposes mTORC1 activity in germ-line progenitor cells by inducing the expression of REDD1, an mTORC1 inhibitor (44). We therefore evaluated whether REDD1 may mediate the effects of KLK4 on mTORC1 via PLZF in PCa cells. We first compared REDD1 levels in LN-shKLK4 and LN-Scr cells. There was a significant increase in REDD1 expression, at both mRNA and protein levels, upon KLK4 knockdown (Fig. 6 *A* and *B*). Furthermore, knockdown of PLZF in LN-shKLK4 cells significantly reduced REDD1 expression, accompanied by an increase in pS6K levels (Fig. 6*C*). Similarly, in LNCaP cells, whereas PLZF knockdown reduced REDD1 expression and mTOR activation (Fig. 6*D* and Fig. S11), ectopic expression of PLZF increased it (Fig. 6*E*). These obser-

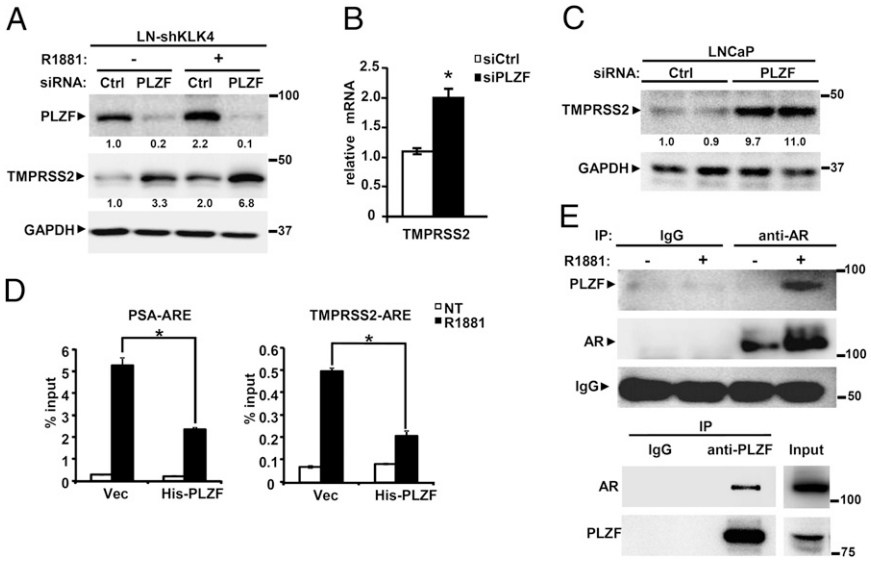

Fig. 5. PLZF inhibits AR signaling in PCa cells. (*A* and *B*) Knockdown of PLZF in LN-shKLK4 cells restores AR signaling. LN-shKLK4 cells were transfected with a scrambled siRNA (siCtrl) or siRNA against PLZF (siPLZF). Two days after transfection, cells were harvested and used in Western (*A*) or qPCR (*B*) analysis for TMPRSS2 expression. Relative quantification of band intensities are indicated below the lanes; intensity of the sample in the Ctrl siRNA lane was set to 1.0. Error bars indicate SD ($n = 3$); $^*P < 0.05$. (*C*) Knockdown of PLZF in LNCaP cells induces AR target gene TMPRSS2 expression. LNCaP cells were treated with siCtrl or siPLZF. Two days after transfection, cells were harvested for Western analysis using the indicated antisera. Relative quantification of band intensities are indicated below the lanes; intensity of sample in the first Ctrl siRNA lane was set to 1.0. (*D*) PLZF decreases AR binding to its response elements in vivo. LNCaP cells expressing vector control or His-PLZF were grown in RPMI supplemented with charcoal-stripped serum for 2 d, followed by 10 nM R1881 treatment for 24 h. ChIP assay was performed using an AR antibody. Error bars indicate SD ($n = 3$); $^*P < 0.05$. (*E*) PLZF interacts with AR in vivo. Immunoprecipitation was conducted in LNCaP cells using AR (*Upper*) or PLZF antiserum (*Lower*), and rabbit IgG was used as a negative control. Precipitated fractions were subjected to Western analysis using either the AR or PLZF antisera. All experiments were repeated three times with consistent results.

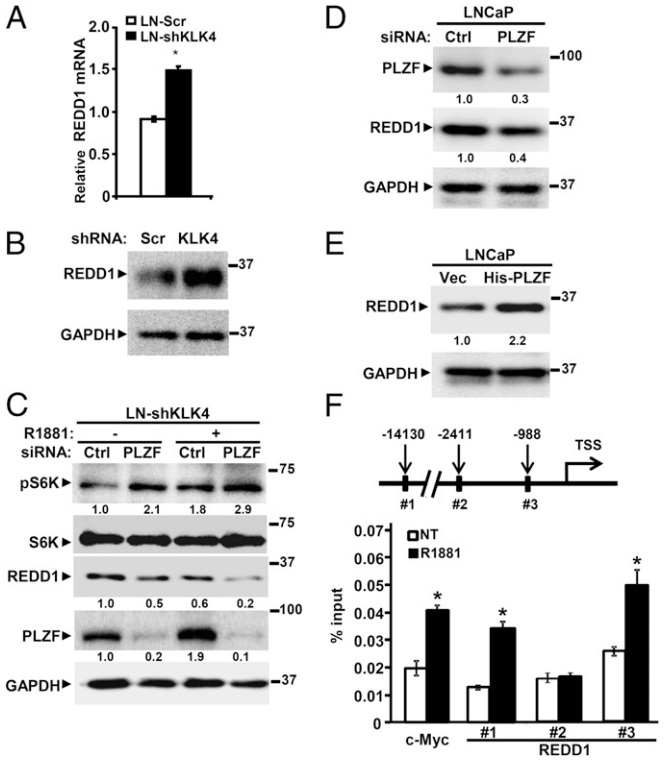

Fig. 6. KLK4 regulates REDD1 expression and mTORC activity through PLZF. (*A* and *B*) Knockdown of KLK4 significantly increases REDD1 expression. REDD1 expression in LN-Scr and LN-shKLK4 cells were determined by qPCR (*A*) and Western (*B*) analyses. Error bars indicate SD ($n = 3$); $^*P < 0.01$. (*C* and *D*) PLZF is required for REDD1 expression. siRNA mediated knockdown of PLZF was performed in LN-shKLK4 cells (*C*) or LNCaP cells (*D*), and expression of REDD1, S6K, and pS6K were determined by Western analyses. Relative quantification of band intensities are indicated below the lanes; intensity of the sample in the Ctrl siRNA lane was set to 1.0. (*E*) Ectopic expression of PLZF increases REDD1 expression. LNCaP cells stably expressing His-PLZF or vector control (Vec) were harvested and used in Western analysis for REDD1 expression. All experiments were repeated at least three times with similar results. Relative quantification of band intensities are indicated below the lanes; intensity of the sample in the Vec lane was set to 1.0. (*F*, *Upper*) Using online bioinformatics tools, three putative PLZF binding sites were predicted in the REDD1 5′ flanking region (up to 20-kb upstream of translation start site). Numbers indicate the starting position of the putative binding sites. Positions of ChIP amplicons are indicated. (*Lower*) LNCaP cells were grown in RPMI supplemented with charcoal-stripped serum for 2 d, followed by R1881 (10 nM) treatment for 24 h. ChIP was performed using a PLZF antibody. Error bars indicate SD ($n = 3$); $^*P < 0.05$. All experiments were repeated at least two times with consistent results.

vations documented that PLZF is required for REDD1 expression in LNCaP cells. In mouse germ-line progenitor cells, PLZF regulates REDD1 transcription through binding to the REDD1 gene (44). To examine whether PLZF similarly regulates REDD1 expression in PCa cells, we analyzed the upstream region of the human REDD1 gene using bioinformatics tools and found three putative PLZF binding sites. ChIP analysis showed that PLZF is recruited to two of these sites in response to androgen, similar in magnitude as in the previously identified PLZF site in the c-Myc promoter (44, 45) (Fig. 6*F*). These data indicate that PLZF binds directly to at least two sites in the REDD1 gene and regulates its expression in PCa cells.

Therapeutic Targeting of KLK4 by Nanoliposomal siRNA Reverses in Vivo Tumor Growth. The data presented above showed that KLK4 promotes proliferation, colony formation, survival, tumor growth, and progression of PCa. However, the role of KLK4 in tumorigenesis and the therapeutic potential of its knockdown, if any, is not known. To assess this possibility, KLK4 was silenced using systemically administered nanoliposomal siRNA in nude mice carrying xenografted tumors of LNCaP or VCaP cells. Tumors were first grown to ∼3–5 mm in size, upon which mice were given nanoliposome encapsulated nonsilencing control siRNA or KLK4 siRNA (150 μg/kg, twice a week) by tail vein injection and tumor growth was followed in time. Using this strategy, it has been established that knockdown rates around 80% can routinely be achieved in similar xenograft experiments (e.g., refs. 46 and 47). Consistently, KLK4 expression in the tumor samples upon nanoliposomal siRNA delivery was decreased by ∼70% (Fig. S12). As shown in Fig. 7 *A* and *B*, whereas upon the empty or control siRNA loaded nanoliposome injection tumors continued to grow rapidly, there was a dramatic and time-dependent reversal of tumor size upon injection of nanoliposomes containing KLK4 siRNA in both preclinical models reaching regression of >90% at the final time points tested. These experiments establish that xenografted human PCa tumor growth can profoundly be reversed by targeting KLK4.

Discussion

AR and PI3K signaling are two of the most frequently activated pathways in a variety of disorders, including the development and progression of PCa (for reviews, see refs. 7, 35, and 39). Furthermore, compensatory cross-talk between these two pathways have been implicated in progression of PCa with PTEN/PI3K dysregulation (3, 5, 48). Thus, these pathways are currently two of the main targets for the development of novel PCa treatment options where synergetic inhibition of AR and PI3K/mTOR signaling is the goal (3, 5, 48) (for a review, see ref. 35). Here we have described a unique molecular switch, at the center of which is KLK4–PLZF interaction, which regulates both AR and mTORC1 signaling. The data we presented suggest that targeting of this molecular switch may be a novel approach for PCa therapy.

A recent genomic profiling of human PCa samples integrating alterations in expression, DNA copy number, and mutations suggested that the three key pathways to target in PCa are AR, PI3K, and RAF/MEK signaling, consistent with previous findings (39). Among these pathways, androgen signaling has been shown to regulate proliferation and inhibit apoptosis in all phases of PCa, even in CRPC after androgen ablation therapy; the growth of this advanced stage of the disease still depends on AR, which is either overexpressed or is activated through various alternative mechanisms (3, 4, 7, 49). Therefore, AR remains a critical therapeutic target for PCa, for which there are extensive efforts to develop reagents that effectively inhibit its expression and activity (50). We found that KLK4 is required for AR-dependent gene expression, at least in part by regulating AR expression (Fig. 2).

Studies on murine Klk4 have shown that it has direct roles in tooth formation and this involves its protease function (51). No other phenotype has been reported for Klk4 knock-out mice, although their prostate biology or the consequence of Klk4 knockout in a transgenic prostate cancer model has not been explored to date. The data we present here predict that these mice would have AR-associated pathologies and may be less prone to develop prostate anomalies when challenged. Our findings also suggest that the protease activity of KLK4 may not be required for its biological effects in the normal prostate and prostate cancer and thus may be different compared with other tissues, such as the tooth. Further work is required to test these possibilities.

The available AR inhibitors have limited effects and thus additional approaches to target AR signaling are being explored, including some compounds in phase I/II clinical trials (for reviews, see refs. 7 and 50). The data we have presented here suggest that KLK4 may be a unique target for PCa therapy because of its essential role in AR levels and activity (Fig. 2). As KLK4 physically interacts with PLZF and inhibits its expression (Figs. 3 and 4), and

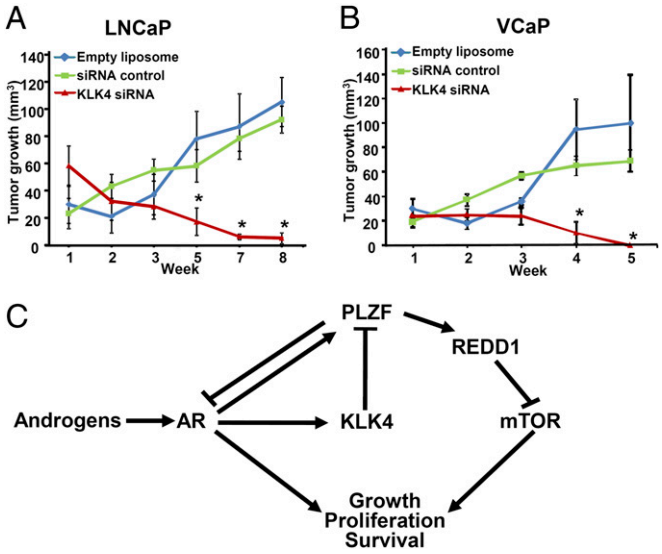

Fig. 7. Therapeutic efficacy of KLK4 silencing in preclinical models of prostate cancer. Tumor xenografts were established by subcutaneous injection of LNCaP (*A*) or VCaP (*B*) cells into the right flank of male nude mice. After tumors have grown to 3–5 mm in size in about 2 wk, mice were given nanoliposome encapsulated nonsilencing control siRNA or KLK4 siRNA from the tail vein, twice a week (150 μg/kg) and the tumor sizes were measured every week. Error bars indicate SEM; $*P < 0.05$. (*C*) Model depicting interactions between AR, KLK4, and PLZF, and the functional consequences for PCa. AR activates PLZF expression which negatively regulates AR levels/activity, as well as suppressing mTORC1 function through increasing REDD1 expression. AR also activates KLK4 expression, which maintains AR signaling by opposing PLZF activity and expression. Overexpression of KLK4 or dysregulation of PLZF will result in sustained activation of the AR and mTOR signaling pathways, which leads to increased proliferation and survival of PCa cells.

because PLZF suppresses AR activity in PCa cells (Fig. 5), inhibition of KLK4 to hinder AR signaling makes this a unique pathway for consideration as a therapeutic target in PCa.

In addition to AR signaling, we have found that the PI3K pathway is also significantly affected by KLK4. PI3K signaling has been implicated in the development of various human cancers, including PCa (9–11, 18). PI3K activation is negatively regulated by the tumor-suppressor PTEN, which is frequently deleted in PCa, and dysregulation of the PTEN/PI3K pathway has also been associated with the development of castration-resistant disease, both in mouse PCa models (48) and human PCa (52). Inhibition of this pathway by various approaches, such as PTEN restoration and small molecular inhibitors against AKT, induces growth arrest and enhances apoptosis in LNCaP cells, which are PTEN-null, as well as in other PCa cell lines (21, 53). However, our previous observations in LNCaP cells showed that inhibition of PI3K pathway activated AR transcriptional activity (54). Inhibition of AR signaling by the PI3K pathway was also demonstrated in PCa mouse models by two recent independent studies (3, 5), which suggested that PTEN loss represses AR signaling through either regulation of early growth response protein 1 (EGR1)/c-Jun/enhancer of zeste homolog 2 (EZH2) or suppression of human epidermal growth factor receptor (HER) 2/3. Moreover, both studies presented evidence that blocking AR leads to activation of PI3K through reducing the AR target FK506 binding protein 5 (FKBP5) to destabilize PH domain and leucine rich repeat protein phosphatase (PHLPP), a phosphatase that inactivates pAKT. These observations established the existence of reciprocal feedback regulation of PI3K and AR signaling, the two most frequently activated signaling pathways, in prostate cancers, suggesting that cotargeting both pathways in PCa may enhance therapeutic efficacy. The data we provide here show that this is exactly what KLK4 targeting can achieve, by both inhibiting AR and mTORC1 signaling. Because KLK4 is highly prostate-enriched, this would also limit any potential deleterious effects in other tissues.

On the basis of the data presented herein, we propose the following model (Fig. 7*C*): AR activation induces both KLK4 and PLZF expression, as well as cell proliferation and survival. Rapid induction of PLZF suppresses AR transcriptional activity through direct interaction with AR, but induction of KLK4 negatively regulates PLZF stability/activity, again through direct interactions. Furthermore, KLK4 is required for AR steady state levels. This model predicts that AR activity is under tight control of PLZF and KLK4 levels. When there is higher level of PLZF, AR signaling is restrained, whereas when KLK4 levels are higher, AR signaling is active, cell proliferation is increased, and apoptosis is inhibited. In addition to these effects on AR, in parallel, KLK4 positively impacts the mTORC1 complex by inhibiting PLZF from activating REDD1, which relieves mTORC1 inhibition and finally leads to cell proliferation. In light of the cross-talk between the AR and mTOR signaling (3, 5, 54), KLK4 affects both pathways and overrides any compensatory cross-talk. Thus, KLK4 has a central role in maintaining the activity of this circuit impacting both AR and mTOR signaling, thereby ensuring cell growth, proliferation, and survival. Taken together, our results suggest that KLK4 is a central component of a molecular switch that could be a novel therapeutic target for PCa treatment.

Materials and Methods

Ethics Statement. Primary human prostate tumor patient specimens were obtained from patients providing informed consent under protocols approved by the Oslo University Hospital Review Boards. All animal experiments were performed in accordance with Oslo University Hospital or MD Anderson Cancer Center Animal Care and Use Committee-approved protocol. Per institution practices, nude mice were used in the experiments carried out at MD Anderson and NOD/SCID mice at Oslo University Hospital.

Cell Culture. LNCaP and 293T cells were obtained from ATCC and routinely maintained under standard conditions. Human PCa cell line VCaP was a kind gift of Frank Smit (Radboud University Nijmegen Medical Centre, Nijmegen, The Netherlands). Human PCa cell line LAPC4 was a kind gift of Robert Reiter (Clark Urological Center, University of California, Los Angeles, CA). The response of PCa cells to androgen treatment for growth, as well as androgen-mediated gene expression, was determined to authenticate the cell lines.

Plasmids. The pLKO.1 shRNA vectors used to knockdown KLK4 or PLZF were purchased from Open Biosystems (Thermo Fisher Scientific). KLK4 mutant was generated from pcDNA4-HisMax-KLK4 with GeneTailor Site-Directed Mutagenesis System (Invitrogen). Lentiviral vectors for overexpressing KLK4 and PLZF were generated from pGIPZ (Open Biosystems, Thermo Fisher Scientific) by removing shRNA coding fragment and replacing the GFP ORF (pGIPZ) with the desired ORF.

Generation of Stable Knockdown Cells. Lentivirus particles were produced in 293T cells according to the manufacturer's instructions. To generate stable cell lines, cells were transduced by lentivirus and the stable knockdown or overexpression cells were obtained by selection with puromycin. After selection, the established stable cell lines were maintained in growth medium containing 0.2 μg/mL puromycin.

RNA Extraction, cDNA Synthesis, and qPCR. Total RNA from cells or frozen prostate tissue was extracted using TRIzol reagent (Invitrogen) according to the manufacturer's protocol. The RNA concentration was measured by Nanodrop ND-1000 spectrophotometer, and RNA quality was verified by agarose gel electrophoresis. The cDNA synthesis was performed using SuperScript II Reverse Transcriptase (Invitrogen), which was then used as template in qPCR with SYBR green dye and LightCycler 480 system (Roche). The sequences of the primers used are available upon request. The TATA binding protein (*TBP*) expression was used for normalization.

Western Analysis. At the indicated time points, cells were harvested and whole-cell extracts were prepared and subjected to Western analysis as

described previously (26). Rabbit polyclonal anti-KLK4 was described previously (26). Antisera against cleaved caspase-3, cleaved PARP, phospho-Akt (Ser473), phospho-Akt (Thr307), total Akt, phospho-p70S6K (Thr389), total p70S6K, phospho-mTOR (Ser2448), total mTOR, phospho-ERK1/2 (Thr202/Tyr204), total ERK1/2, phospho-p65 (Ser536), and total p65 (Cell Signaling Technology), PSA, AR (N20), PLZF (D-9), and PLZF (H-300) (Santa Cruz Biotechnology), TMPRSS2 (Epitomics), REDD1 (Proteintech), β-actin, GAPDH, and secondary antisera conjugated to horseradish peroxidase (Sigma) were used according to the manufacturer's instructions. Band intensities were determined by densitometry.

Cell Proliferation Assay. Cells were seeded in six-well plates at 25,000 cells per well in RPMI-1640 medium containing 10% (vol/vol) FBS and the cell number was determined at the indicated time points using a hemocytometer.

Soft-Agar and Clonogenic Assays. Anchorage-independent growth was assessed with the soft agar assay. Briefly, six-well plates were first plated with RPMI-1640 medium containing 10% (vol/vol) FBS and 0.8% agar. Next, 2,000 cells were suspended in RPMI-1640 medium containing 10% (vol/vol) FBS and 0.3% agar, and the cell suspension was plated on top of the first layer. Top agar was covered with culture medium and the plates were maintained in the tissue-culture incubator. Medium was changed twice a week and cells were cultured for 3 wk. After washing twice with PBS, the colonies formed were visualized with 0.5 mL of 0.01% Crystal violet and photographed.

Reporter Gene Assay. LNCaP cells were grown in six-well plates and were transiently transfected with the AR-dependent reporter construct -285-PB-LUC as described previously (54). After 6 h of transfection, cells were given phenol red-free medium supplemented with 0.5% charcoal treated serum and R1881 (to 10 nM) was added as indicated. Twenty-four hours later cells were harvested and luciferase assay was performed.

The effect of PLZF on AR transcriptional activity was determined in HeLa cells. Briefly, cells were cotransfected with 100 ng AR-dependent reporter -285-PB-LUC, 10 ng PSG5-AR construct, and indicated amounts of pCDNA4-HM-PLZF or empty vector. Twenty-four hours after transfection, cells were treated with 10 nM R1881 for 2 d and luciferase assay was performed.

Xenografts in NOD/SCID Mice. Assay of tumor growth in NOD/SCID Il2Rg^{null} mice (strain NOD.Cg-Prkdc^{scid} Il2rg^{tm1Wjl}/SzJ, 5–8 wk of age) was performed as described previously (55). Briefly, three million cells were suspended in 50 μL RPMI-1640 medium and mixed with 50 μL Matrigel (BD Biosciences). The mixture was then subcutaneously inoculated into male mice in both hind flanks. Tumor size was measured weekly in two dimensions with calipers and the tumor volume V was calculated according to the formula: $V = W^2 \times L \times 0.5$, where W and L are tumor width and length, respectively. All studies were conducted according to an experimental protocol approved by the Oslo University Hospital Institutional Animal Care and Use Committee.

Cell Cycle Analysis. Cells were synchronized at the G0/G1 phase by serum starvation for 48 h and then released into the cell cycle by readdition of 10% FBS in the medium. After 16 h, cells were trypsinized, washed with PBS, and then fixed in 70% (vol/vol) ice-cold ethanol for 2 h at 4 °C. To assess the cell-cycle profile, fixed cells were treated with RNase A, stained with propidium iodide, and were analyzed by flow cytometry (Becton Dickinson).

Apoptosis Assays. Apoptosis and the treatments for its induction and detection were as described previously (55). To detect proapoptotic factor-induced apoptosis, cells were treated with 50 ng/mL TRAIL (Enzo Life Sciences), 20 μM LY294002 (Invitrogen), or a combination of both agents for indicated times. Extent of apoptosis was then detected by TUNEL or flow cytometry analysis. Briefly, DeadEnd Fluorometric TUNEL system (Promega) was used according to the manufacturer's instructions. Vectashield HardSet Mounting Medium with DAPI (Vector Laboratories) was used to mount the sections and to visualize cell nuclei. Fluorescence was observed using an Axioplan2 imaging microscope (Zeiss) at a magnification of 20×, and pictures were taken with an AxioCam MR3_2 camera (Zeiss). A minimum of 3,000 cells per data point were counted, and the number of TUNEL-positive cells was expressed as a percentage of the total number of cells.

Coimmunoprecipitation. The interaction between PLZF and KLK4 was analyzed by co-IP. Briefly, COS-7 cells were cotransfected with plasmids including pcDNA4-HA-KLK4 with pCDNA4-HM-PLZF, pCDNA4-BR or pCDNA4-HM-RD. Two days posttransfection, cells were harvested and lysed in IP buffer (20 mM Tris·HCl, pH 7.5, 150 mM NaCl, 0.5% Triton-X100, 1 mM EDTA, 1 mM EGTA, 1 mM DTT and protease inhibitors). The lysate was cleared by centrifugation and supernatant was incubated with anti-His antibody for overnight at 4 °C, followed by a 2-h incubation at 4 °C with protein A-coupled agarose beads. Complexes were washed three times with IP buffer and then subjected to SDS/PAGE and Western analysis. To assess the interaction of endogenous proteins, co-IP of PLZF and AR, or PLZF and KLK4, was conducted with LNCaP cells, and IP was performed with anti-AR polyclonal antibody or anti-PLZF polyclonal antibody as indicated.

Patient Material. Primary tumors from 37 patients with clinically localized PCa, consecutively diagnosed and primarily treated with radical prostatectomy at the Portuguese Oncology Institute, Porto, Portugal, were prospectively collected. In five radical prostatectomy specimens with PCa, high-grade prostatic intraepithelial neoplasia lesions were identified and separately procured for analysis. For control purposes, BPH samples were obtained from 11 randomly selected patients that underwent transurethral resection of the prostate. Five-micrometer-thick sections were cut and stained for the identification of the areas of PCa, high-grade prostatic intraepithelial neoplasia, and BPH.

Immunohistochemistry. Specimen preparation and immunohistochemistry were performed as described previously (29, 56). The study was approved by the South-East Norway Health Authority Regional Ethics Committee.

Analysis of Human PCa Gene-Expression Profiles. To assess the relevance of our findings to expression in human PCas, we examined the possible correlation of AR target genes with KLK4 expression level. A gene expression profile (6,100 genes included) of 281 cases from the population-based Swedish-Watchful Waiting cohort was used in this analysis (37). The samples were categorized in two groups designed as Low_KLK4 and High_KLK4, using the mean of the expression for the gene KLK4 as the threshold. The differential expression of each gene between Low_KLK4 and High_KLK4 groups was expressed as $\log_2$ of the fold-change. The expression of a battery of direct AR target genes identified in a recent report were used (36). A PCa gene expression profile dataset available at the cBio Cancer Genomics Portal (39) was used for the secondary validation scheme.

Chromatin Immunoprecipitation. ChIP experiments were carried out according to the standard protocol (Upstate Biotechnology) with some modifications. Briefly, cells were treated as indicated before cross-linking with 1% formaldehyde at 37 °C. The cells were then quenched with 125 mM glycine. Chromatin was sheared using the Bioruptor sonicator (Diagenode). After centrifugation, sheared chromatin was immunoprecipitated overnight with an AR polyclonal antibody, PLZF polyclonal antibody, or rabbit IgG. Antibody-bound chromatin complexes were then immunoprecipitated with protein A-agarose beads, and eluted in SDS buffer. Formaldehyde cross-linking was reversed at 65 °C overnight, followed by DNA purification. Immunoprecipitated DNA, as well as input DNA, was quantified by qPCR using specific primer sets as indicated. Primer sequences are available upon request.

Nanoliposomal siRNA Targeting of PCa Xenografts. Liposomal siRNA for in vivo delivery was prepared as described previously (46). Briefly, siRNA was incorporated into dioleoyl-sn-glycero-3-phosphocholine (DOPC). DOPC and siRNA were mixed in the presence of excess tertiary butanol at a ratio of 1:10 (wt/wt) siRNA/DOPC. Tween 20 was added to the mixture in a ratio of 1:19 Tween 20:siRNA/DOPC. The mixture was vortexed, frozen in an acetone/dry ice bath, and lyophilized. The amount of siRNA incorporated by liposomes was calculated and entrapment capacity was found to be around 90%. To eliminate the quantity of siRNA not taken up by liposomes, free siRNA was separated from liposomes using 30,000 nominal molecular weight-limit filter units (Millipore). The mean size of the liposomes was determined by light scattering (Zetasizer nano ZS) and found to be about 65 nm.

For in vivo therapeutic targeting of KLK4 by systemically administered nanoliposomal siRNA, athymic male nu/nu mice (5-wk old) were obtained from the Department of Experimental Radiation Oncology at MD Anderson Cancer Center. The mice were housed five per cage in standard acrylic glass cages in a room maintained at constant temperature and humidity with a 12-h light/dark cycle; they were fed a regular autoclaved chow diet and water ad libitum. All studies were conducted according to an experimental protocol approved by the MD Anderson Institutional Animal Care and Use Committee. LNCaP cells or VCaP cells (2×10^6) were injected subqutaneously into the right flank of each mouse with 10% matrigel. Once tumors reached 3–5 mm in size, mice were given nanoliposome encapsulated nonsilencing control siRNA or KLK4 siRNA 150 μg/kg (~4 μg siRNA per mouse), twice a week from the tail vein in 100 μL saline. At the indicated time points, the tumor volumes

were measured. At the end of 5 and 8 wk of nanoliposomal siRNA treatment for VCaP and LNCaP tumors, respectively, tumor were harvested and examined by H&E staining and qPCR analyses.

Statistics. Statistical comparisons were made with the Student *t* test. A value of $P < 0.05$ was considered indication of statistical significance.

ACKNOWLEDGMENTS. We thank Frank Smit and Robert Reiter for cell lines; Jorma Palvimo for the reporter plasmid; Bjørn Risberg for pathology help; and the members of the F.S. laboratory for helpful discussions and critically reading the manuscript. This work was supported by grants from the University of Oslo, Norwegian Research Council, Anders Jahre Fund, and Norwegian Cancer Society (to F.S.).

1. Jemal A, et al. (2011) Global cancer statistics. *CA Cancer J Clin* 61(2):69–90.
2. Reddy GP, et al. (2006) Regulatory processes affecting androgen receptor expression, stability, and function: Potential targets to treat hormone-refractory prostate cancer. *J Cell Biochem* 98(6):1408–1423.
3. Carver BS, et al. (2011) Reciprocal feedback regulation of PI3K and androgen receptor signaling in PTEN-deficient prostate cancer. *Cancer Cell* 19(5):575–586.
4. Edwards J, Krishna NS, Grigor KM, Bartlett JM (2003) Androgen receptor gene amplification and protein expression in hormone refractory prostate cancer. *Br J Cancer* 89(3):552–556.
5. Mulholland DJ, et al. (2011) Cell autonomous role of PTEN in regulating castration-resistant prostate cancer growth. *Cancer Cell* 19(6):792–804.
6. Kumar-Sinha C, Tomlins SA, Chinnaiyan AM (2008) Recurrent gene fusions in prostate cancer. *Nat Rev Cancer* 8(7):497–511.
7. Chen Y, Sawyers CL, Scher HI (2008) Targeting the androgen receptor pathway in prostate cancer. *Curr Opin Pharmacol* 8(4):440–448.
8. Zegarra-Moro OL, Schmidt LJ, Huang H, Tindall DJ (2002) Disruption of androgen receptor function inhibits proliferation of androgen-refractory prostate cancer cells. *Cancer Res* 62(4):1008–1013.
9. Vivanco I, Sawyers CL (2002) The phosphatidylinositol 3-Kinase AKT pathway in human cancer. *Nat Rev Cancer* 2(7):489–501.
10. Samuels Y, et al. (2004) High frequency of mutations of the PIK3CA gene in human cancers. *Science* 304(5670):554.
11. Li J, et al. (1997) PTEN, a putative protein tyrosine phosphatase gene mutated in human brain, breast, and prostate cancer. *Science* 275(5308):1943–1947.
12. Cully M, You H, Levine AJ, Mak TW (2006) Beyond PTEN mutations: The PI3K pathway as an integrator of multiple inputs during tumorigenesis. *Nat Rev Cancer* 6(3):184–192.
13. Trotman LC, et al. (2003) Pten dose dictates cancer progression in the prostate. *PLoS Biol* 1(3):E59.
14. Di Cristofano A, Pandolfi PP (2000) The multiple roles of PTEN in tumor suppression. *Cell* 100(4):387–390.
15. Abate-Shen C, Shen MM (2000) Molecular genetics of prostate cancer. *Genes Dev* 14(19):2410–2434.
16. Wang S, et al. (2003) Prostate-specific deletion of the murine Pten tumor suppressor gene leads to metastatic prostate cancer. *Cancer Cell* 4(3):209–221.
17. Sengupta S, Peterson TR, Sabatini DM (2010) Regulation of the mTOR complex 1 pathway by nutrients, growth factors, and stress. *Mol Cell* 40(2):310–322.
18. Dancey J (2010) mTOR signaling and drug development in cancer. *Nat Rev Clin Oncol* 7(4):209–219.
19. Wullschleger S, Loewith R, Hall MN (2006) TOR signaling in growth and metabolism. *Cell* 124(3):471–484.
20. Ayala G, et al. (2004) High levels of phosphorylated form of Akt-1 in prostate cancer and non-neoplastic prostate tissues are strong predictors of biochemical recurrence. *Clin Cancer Res* 10(19):6572–6578.
21. Engelman JA (2009) Targeting PI3K signalling in cancer: Opportunities, challenges and limitations. *Nat Rev Cancer* 9(8):550–562.
22. DeYoung MP, Horak P, Sofer A, Sgroi D, Ellisen LW (2008) Hypoxia regulates TSC1/2-mTOR signaling and tumor suppression through REDD1-mediated 14-3-3 shuttling. *Genes Dev* 22(2):239–251.
23. Vega-Rubin-de-Celis S, et al. (2010) Structural analysis and functional implications of the negative mTORC1 regulator REDD1. *Biochemistry* 49(11):2491–2501.
24. Velasco AM, et al. (2004) Identification and validation of novel androgen-regulated genes in prostate cancer. *Endocrinology* 145(8):3913–3924.
25. Lai J, et al. (2010) A variant of the KLK4 gene is expressed as a *cis* sense-antisense chimeric transcript in prostate cancer cells. *RNA* 16(6):1156–1166.
26. Xi Z, et al. (2004) Kallikrein 4 is a predominantly nuclear protein and is overexpressed in prostate cancer. *Cancer Res* 64(7):2365–2370.
27. Korkmaz KS, Korkmaz CG, Pretlow TG, Saatcioglu F (2001) Distinctly different gene structure of KLK4/KLK-L1/prostase/ARM1 compared with other members of the kallikrein family: Intracellular localization, alternative cDNA forms, and Regulation by multiple hormones. *DNA Cell Biol* 20(7):435–445.
28. Dong Y, et al. (2005) Compartmentalized expression of kallikrein 4 (KLK4/hK4) isoforms in prostate cancer: Nuclear, cytoplasmic and secreted forms. *Endocr Relat Cancer* 12(4):875–889.
29. Klokk TI, et al. (2007) Kallikrein 4 is a proliferative factor that is overexpressed in prostate cancer. *Cancer Res* 67(11):5221–5230.
30. Obiezu CV, et al. (2005) Human kallikrein 4: Quantitative study in tissues and evidence for its secretion into biological fluids. *Clin Chem* 51(8):1432–1442.
31. Veveris-Lowe TL, et al. (2005) Kallikrein 4 (hK4) and prostate-specific antigen (PSA) are associated with the loss of E-cadherin and an epithelial-mesenchymal transition (EMT)-like effect in prostate cancer cells. *Endocr Relat Cancer* 12(3):631–643.
32. Suliman BA, Xu D, Williams BR (2012) The promyelocytic leukemia zinc finger protein: Two decades of molecular oncology. *Front Oncol* 2:74.
33. Yu R, Mandlekar S, Ruben S, Ni J, Kong ANT (2000) Tumor necrosis factor-related apoptosis-inducing ligand-mediated apoptosis in androgen-independent prostate cancer cells. *Cancer Res* 60(9):2384–2389.
34. Chen X, et al. (2001) Constitutively active Akt is an important regulator of TRAIL sensitivity in prostate cancer. *Oncogene* 20(42):6073–6083.
35. Bluemn EG, Nelson PS (2012) The androgen/androgen receptor axis in prostate cancer. *Curr Opin Oncol* 24(3):251–257.
36. Massie CE, et al. (2011) The androgen receptor fuels prostate cancer by regulating central metabolism and biosynthesis. *EMBO J* 30(13):2719–2733.
37. Sboner A, et al. (2010) Molecular sampling of prostate cancer: A dilemma for predicting disease progression. *BMC Med Genomics* 3:8.
38. Kaarbø M, Klokk TI, Saatcioglu F (2007) Androgen signaling and its interactions with other signaling pathways in prostate cancer. *Bioessays* 29(12):1227–1238.
39. Taylor BS, et al. (2010) Integrative genomic profiling of human prostate cancer. *Cancer Cell* 18(1):11–22.
40. Agoulnik IU, Weigel NL (2006) Androgen receptor action in hormone-dependent and recurrent prostate cancer. *J Cell Biochem* 99(2):362–372.
41. Chen Z, et al. (1993) Fusion between a novel Krüppel-like zinc finger gene and the retinoic acid receptor-alpha locus due to a variant t(11;17) translocation associated with acute promyelocytic leukaemia. *EMBO J* 12(3):1161–1167.
42. Jiang F, Wang Z (2004) Identification and characterization of PLZF as a prostatic androgen-responsive gene. *Prostate* 59(4):426–435.
43. Shaknovich R, et al. (1998) The promyelocytic leukemia zinc finger protein affects myeloid cell growth, differentiation, and apoptosis. *Mol Cell Biol* 18(9):5533–5545.
44. Hobbs RM, Seandel M, Falciatori I, Rafii S, Pandolfi PP (2010) Plzf regulates germline progenitor self-renewal by opposing mTORC1. *Cell* 142(3):468–479.
45. McConnell MJ, et al. (2003) Growth suppression by acute promyelocytic leukemia-associated protein PLZF is mediated by repression of c-myc expression. *Mol Cell Biol* 23(24):9375–9388.
46. Landen CN, Jr., et al. (2005) Therapeutic EphA2 gene targeting in vivo using neutral liposomal small interfering RNA delivery. *Cancer Res* 65(15):6910–6918.
47. Nick AM, et al. (2011) Silencing of p130cas in ovarian carcinoma: A novel mechanism for tumor cell death. *J Natl Cancer Inst* 103(21):1596–1612.
48. Zhang W, et al. (2009) Inhibition of tumor growth progression by antiandrogens and mTOR inhibitor in a Pten-deficient mouse model of prostate cancer. *Cancer Res* 69(18):7466–7472.
49. Linja MJ, et al. (2001) Amplification and overexpression of androgen receptor gene in hormone-refractory prostate cancer. *Cancer Res* 61(9):3550–3555.
50. Taplin ME (2007) Drug insight: role of the androgen receptor in the development and progression of prostate cancer. *Nat Clin Pract Oncol* 4(4):236–244.
51. Simmer JP, Hu Y, Lertlam R, Yamakoshi Y, Hu JC (2009) Hypomaturation enamel defects in Klk4 knockout/LacZ knockin mice. *J Biol Chem* 284(28):19110–19121.
52. Ham WS, et al. (2009) Pathological effects of prostate cancer correlate with neuroendocrine differentiation and PTEN expression after bicalutamide monotherapy. *J Urol* 182(4):1378–1384.
53. Sarker D, Reid AH, Yap TA, de Bono JS (2009) Targeting the PI3K/AKT pathway for the treatment of prostate cancer. *Clin Cancer Res* 15(15):4799–4805.
54. Kaarbø M, et al. (2010) PI3K-AKT-mTOR pathway is dominant over androgen receptor signaling in prostate cancer cells. *Cell Oncol* 32(1-2):11–27.
55. Wang L, et al. (2010) STAMP1 is both a proliferative and an antiapoptotic factor in prostate cancer. *Cancer Res* 70(14):5818–5828.
56. Xi Z, et al. (2004) Kallikrein 4 is associated with paclitaxel resistance in ovarian cancer. *Gynecol Oncol* 94(1):80–85.